International Journal of Innovative Engineering Applications

Journal homepage: https://dergipark.org.tr/ijiea

INVESTIGATION OF THE IMPACT OF POROUS STRUCTURE GEOMETRY AND FLOW CHARACTERISTICS ON HEAT TRANSFER EFFECTIVENESS IN A SHELL-AND-TUBE HEAT EXCHANGER

***Mahir Sahin*[*1], *Mustafa Kilic*[1], *Murat Gokcek*[2]**

[1]*Adana Alparslan Türkeş Science and Technology University, Faculty of Engineering, Mechanical Engineering Department, Adana, Turkey*
[2]*Niğde Ömer Halisdemir University, Faculty of Engineering, Mechanical Engineering Department, Niğde, Turkey*

Abstract

Original scientific paper

The present study investigates the effects of Reynolds number, fluid inlet temperature, porosity ratio, and porous thickness on the heat transfer effectiveness of a shell-and-tube heat exchanger operating under laminar flow conditions. The primary objective of the study is to determine how these parameters influence thermal performance and to establish a clear understanding of their roles in enhancing heat transfer effectiveness. The investigated parameters are Reynolds numbers of 1000, 2000, 3000, and 4000; inlet temperatures of 25°C, 30°C, 35°C, and 40°C; porosity ratios of 0.5, 0.6, 0.8, and 0.9; and porous thicknesses of 5/80, 10/80, 15/80, and 20/80. Numerical model validated by experimental data shows that at Re = 1000, the heat transfer effectiveness of pure water at 40°C is 1.1% higher than that at 25°C, while this difference increases to 1.9% at Re = 4000. When the inlet temperature is raised from 25°C to 40°C, the average enhancement in effectiveness is 1.7% for each Re value. At constant inlet temperature, increasing the Reynolds number from 1000 to 4000 improves the heat transfer effectiveness by 12.8%. The results confirm that heat transfer effectiveness (ε) increases with fluid inlet temperature across all Re values. Furthermore, at Re = 1000, a porosity ratio of Φ = 0.9 yields 1.3% higher effectiveness compared to 0.5 at the same temperature. Similarly, for porous thickness L/D (porous thickness/pipe diameter), a structure with 20/80 provides 2.2% higher effectiveness than 5/80 under identical conditions. These findings demonstrate that optimizing porosity and porous thickness, along with flow and temperature parameters, can significantly enhance heat transfer performance. The results indicate that shell-and-tube heat exchangers with porous inserts can be designed to achieve higher thermal effectiveness and improved energy efficiency in future applications.

Keywords: *Heat transfer, Re number, porous structure, heat exchanger, fluid flow.*

GÖVDE BORULU BİR ISI DEĞİŞTİRİCİDE GÖZENEKLİ YAPI GEOMETRİSİ VE AKIŞ ÖZELLİKLERİNİN ISI TRANSFERİ ETKİNLİĞİ ÜZERİNDEKİ ETKİSİNİN İNCELENMESİ

Özet

Orijinal bilimsel makale

Bu çalışma, laminer akış koşulları altında çalışan bir gövde-borulu ısı değiştiricisinde Reynolds sayısı, akışkan giriş sıcaklığı, gözeneklilik oranı ve gözenekli tabaka kalınlığının ısı transfer etkinliği üzerindeki etkilerini incelemektedir. Bu çalışmanın temel amacı, belirlenen parametrelerin ısıl performansı nasıl etkilediğini belirlemek ve ısı transfer etkinliğini artırmadaki rollerini açık bir şekilde ortaya koymaktır. İncelenen parametreler; Reynolds sayıları 1000, 2000, 3000 ve 4000; giriş sıcaklıkları 25°C, 30°C, 35°C ve 40°C; gözeneklilik oranları 0.5, 0.6, 0.8 ve 0.9; ve gözenekli tabaka kalınlıkları 5/80, 10/80, 15/80 ve 20/80 olarak belirlenmiştir. Deneysel verilerle doğrulanan sayısal model, Re = 1000 için 40°C'deki saf suyun ısı transfer etkinliğinin 25°C'deki saf suya göre %1,1 daha yüksek olduğunu, bu farkın Re = 4000'de %1,9'a yükseldiğini göstermiştir. Giriş sıcaklığı 25°C'den 40°C'ye artırıldığında, her Re değeri için etkinlikte ortalama %1,7'lik bir artış elde edilmiştir. Giriş sıcaklığı sabit tutulduğunda, Reynolds sayısının 1000'den 4000'e yükseltilmesi ısı transfer etkinliğini %12,8 oranında artırmıştır. Sonuçlar, tüm Re değerlerinde ısı transfer etkinliğinin (ε) akışkan giriş sıcaklığıyla birlikte arttığını doğrulamaktadır. Ayrıca, Re = 1000 için gözeneklilik oranı Φ = 0,9 olan boruların ısı transfer etkinliği, 0,5 oranına sahip borulara göre aynı sıcaklıkta %1,3 daha yüksektir. Benzer şekilde, L/D (gözenekli yapı kalınlığı/boru çapı) oranı 20/80 oranındaki gözenekli yapı, 5/80 oranındaki yapıya kıyasla %2,2 daha yüksek etkinlik sağlamaktadır. Bu bulgular, gözeneklilik oranı ve gözenekli tabaka kalınlığının yanı sıra akış ve sıcaklık parametrelerinin optimize edilmesiyle ısı transfer performansının önemli ölçüde iyileştirilebileceğini göstermektedir. Elde edilen sonuçlar, gelecekte daha yüksek ısıl etkinliğe ve enerji verimliliğine sahip gövde-borulu ısı değiştiricilerin tasarlanabileceğini ortaya koymaktadır.

Anahtar Kelimeler: *Isı transferi, Re sayısı, gözenekli yapı, ısı değiştiricisi, akışkan akımı.*

*Corresponding author.
E-mail address: msahin@atu.edu.tr (M. Sahin)
Received 14 October 2025; Received in revised form 01 December 2025; Accepted 16 December 2025
 Doi: https://doi.org/10.46460/ijiea.1803466

1 Introduction

Enhancing the performance of heat exchangers plays a crucial role in modern industrial applications, as it directly contributes to both energy efficiency and cost reduction. Improving thermal performance not only ensures better utilization of energy resources but also reduces greenhouse gas emissions, thereby minimizing environmental impacts. Among various enhancement strategies, passive methods are considered highly effective and energy-efficient since they improve heat transfer without requiring additional external power input. Therefore, the development of innovative and energy-efficient heat exchangers has become a key focus area in sustainable engineering and industrial design.

Mohammadi et al. [1] carried out a detailed investigation focusing on the dual objectives of enhancing thermal efficiency and minimizing pressure drop, both of which are essential considerations in the design and optimization of shell-and-tube heat exchangers (STHEs). Their work emphasized that achieving a balance between effective heat transfer and hydraulic performance is critical for efficient system operation. Based on their findings, the configuration with a permeability value of $\varphi = 10^{-9}$ m² demonstrated the most desirable performance characteristics, yielding a significant improvement in heat transfer capability while simultaneously maintaining a minimal pressure drop across the exchanger. Rashidian and Tavakoli [2] conducted a comprehensive study to explore how the inclusion of porous materials influences heat transfer enhancement within heat exchangers. In their research, porous media with different porosity levels, material compositions, and geometric configurations were integrated into the flow passages to analyze their impact on thermal performance. The results demonstrated that the introduction of porous structures within the flow field significantly improved the overall heat transfer characteristics by increasing both the effective thermal conductivity and the apparent heat capacity of the working fluid. This improvement was primarily attributed to the intensified interaction between the fluid and solid matrix, which enhanced energy exchange and promoted a more uniform temperature distribution throughout the exchanger.

Abbasi et al. [3] explored how incorporating porous baffles into a segmental-type shell-and-tube heat exchanger (STHE) affects its thermal performance. The study revealed that introducing porous baffles led to a remarkable enhancement in heat transfer, with an increase of approximately 139% compared to the conventional configuration. However, this improvement was accompanied by a considerable penalty in hydraulic performance, as the pressure drop across the exchanger rose by nearly 247%. Building on similar concepts, Tian et al. [4] constructed a three-dimensional numerical model of an STHE incorporating both porous baffles and porous fins. When compared to a conventional exchanger equipped with solid baffles and no fins, this configuration demonstrated a 65% improvement in pressure drop characteristics and a remarkable 92.14% enhancement in heat transfer capability.

Naqvi and Wang [5] advanced previous research by comparing the thermal and hydrodynamic characteristics of three different shell-and-tube heat exchanger (STHE) configurations—helical, segmental, and clamping anti-vibration baffles—each incorporating porous media on the shell side. These modified designs were evaluated against a conventional segmental STHE lacking porous structures. The findings indicated that increasing porosity from 0.6 to 0.95 led to a reduction in the Nusselt number, while the most favorable thermal performance was obtained at a porous radius ratio of 0.6. Expanding upon the broader significance of optimized porous geometry in heat exchanger design, and providing additional validation of the performance trends identified by Naqvi and Wang, Rad et al. [6] conducted a three-dimensional numerical investigation of an STHE where porous media were individually positioned within the shell and tube domains. Their results demonstrated that the highest heat transfer performance ratio (ζ) on the shell side occurred when the porous radius ratio was maintained at 0.6 and the porosity reached 90%, underscoring that precise control of porous structure geometry can significantly enhance the exchanger's thermal performance.

Marzouk et al. [7] investigated how different baffle geometries—namely conventional single segmental (CSS), hybrid segmental (HS), circular ring (CR), and circular ring with holes (CRH)—affect the thermal performance of shell-and-tube heat exchangers (STHEs) over a newly explored range of Reynolds numbers. Their analysis revealed that the CRH configuration achieved the highest overall effectiveness, outperforming other designs by approximately 166%. Moreover, the CRH arrangement exhibited a 142% higher heat transfer coefficient compared to the traditional CSS configuration. These results highlight the importance of baffle geometry optimization for enhancing convective mixing and flow disturbance, motivating the exploration of alternative perforation and shaping strategies in subsequent studies. In another study, You et al. [8] evaluated the thermo-hydraulic characteristics of a shell-and-tube heat exchanger utilizing trefoil-hole baffles (THB-STHE). The results indicated that the presence of trefoil-shaped perforations effectively minimized the thermal boundary layer thickness adjacent to the wall, thereby substantially improving the overall heat transfer rate within the exchanger.

Bichkhar et al. [9] investigated the reduction of pressure drop on the shell side of a shell-and-tube heat exchanger (STHE) by employing different baffle configurations, namely segmental (SG-STHE), double segmental (DSG-STHE), and continuous helical (CH-STHE), under varying mass flow rates while maintaining identical dimensional parameters. Their results showed that the use of helical baffles significantly reduced the pressure drop compared to the other two types, thereby improving the overall system efficiency. Wen et al. [10] numerically analyzed a shell-and-tube heat exchanger with ladder-type folded baffles and compared its performance with a conventional STHE using plain baffles. The findings revealed that the shell-side heat transfer coefficient increased by 22.3–32.6%, while the overall heat transfer coefficient improved by an average of 21.4%.

Wang et al. [11] developed an innovative shell-and-tube heat exchanger design featuring staggered baffles (ST-STHE), aiming to merge the structural simplicity of the segmental baffle design (SG-STHE) with the superior heat transfer efficiency of the continuous helical baffle configuration (CH-STHE). Their investigation was carried out under uniform mass flow conditions and with a constant number of baffles (n = 9) to ensure consistent comparison. Through parametric evaluation, the study identified the most effective baffle geometries at $\delta = 0.45$ and $\delta = 0.4$, maintaining a staggered inclination angle of $\beta = 90°$, which provided an optimal balance between thermal performance and flow resistance.

In another study, Chen et al. [12] presented a novel shell-and-tube heat exchanger model incorporating triple-layer flower-shaped baffles (TFB-STHE) designed to enhance both mixing and heat transfer characteristics. The findings indicated that increasing the number of blades in the flower-shaped structure contributed to improved flow uniformity and reduced stagnant regions within the shell side. Consequently, this geometric modification led to a more effective energy exchange between the working fluid and the heat transfer surfaces, highlighting the potential of multi-layered baffle configurations in advancing overall thermal performance.

Nie et al. [13] examined whether metal foam baffles could simultaneously reduce pressure loss and increase the outlet–inlet temperature difference in STHEs through proper structural design. Their results showed a 12.9% decrease in pressure drop compared to solid baffles and a 31.0% increase in the outlet–inlet temperature difference. Such findings reinforce the importance of carefully engineered internal structures in improving heat transfer while managing pressure losses. Cao et al. [14] compared the heat transfer characteristics of shell-and-tube heat exchangers equipped with continuous helical and segmental baffles, concluding that the CH-STHE exhibited superior overall thermal performance. Yang and Yang and Liu [15] introduced an alternative shell-and-tube heat exchanger design employing plate-type baffles (PB-STHE) to improve thermal efficiency and flow uniformity within the shell side. Their comparative analysis demonstrated that the plate baffle configuration outperformed the traditional rod baffle (RB-STHE) design in terms of heat transfer capability, as it effectively minimized dead zones and enhanced the overall flow distribution. Together, these observations indicate that careful manipulation of flow pathways through innovative baffle designs can significantly influence the thermal–hydraulic optimization of heat exchangers. He and Li [16] conducted a detailed comparative study between single-tube-pass (STP-STHE) and double-tube-pass (DTP-STHE) heat exchangers by evaluating the pressure drop per unit length and the recovered heat per unit mass of water flowing through the tube side. Their results revealed that the implementation of flower-type baffles provided the most favorable compromise between heat transfer enhancement and required pumping power when compared to conventional segmental and helical baffle arrangements. This outcome highlighted the potential of optimized baffle geometries in improving exchanger performance without imposing excessive hydraulic penalties.

He et al. [17] investigated the boiling heat transfer and two-phase flow characteristics in a shell-and-tube heat exchanger by developing an OpenFOAM-based numerical solver, where the tube bundle was simplified using a porous media model. Their findings show that the predicted void fraction, pressure drop, and temperature distributions exhibit close agreement with experimental benchmarks, demonstrating the applicability of the model for accurate 3D two-phase flow simulations in industrial STHX applications. Riyadi et al. [18] reviewed recent advances in the integration of nanofluids and machine learning for heat transfer improvement in heat exchangers and porous media. Their findings show that machine learning models, particularly SVM, ANN, and genetic algorithms, effectively reduce computational cost, accelerate prediction accuracy, and support optimization of thermal performance for nanofluid-enhanced heat transfer applications. Moraga et al. [19] numerically analyzed unsteady fluid flow and heat transfer in a double-tube heat exchanger with combustion in a porous-filled inner tube, using a finite volume method. The results showed that increasing the Reynolds number of the annular airflow leads to a higher outlet temperature and improved thermal performance, demonstrating a direct link between outer flow Reynolds number and heat transfer enhancement. Qader et al. [20] experimentally investigated heat transfer in a counterflow heat exchanger using porous media and TiO2 nanofluid. Their findings show that combining porous media with TiO2 nanofluid increases heat transfer by over 35%, significantly improving overall effectiveness. Juan and Tao [21] numerically investigated a full-size plate-fin heat exchanger using a porous media model and examined the effects of fluid viscosity and inlet–outlet configuration on flow distribution and pressure drop. Their findings show that increased viscosity enhances flow distribution, and a correlation among flow uniformity, pressure drop, and Reynolds number was established.

Previous research on heat exchangers has primarily utilized porous materials either within the tubes or on their outer surfaces to improve heat transfer performance. Nevertheless, many of these studies have been restricted to narrow ranges of flow and thermal conditions, or have not thoroughly explored the combined influence of multiple porous structural parameters. In this study, the main aim is to evaluate how variations in Reynolds number, inlet temperature, porosity, and porous media thickness collectively affect the thermal behavior under laminar flow conditions. Unlike earlier investigations, this work performs an integrated experimental assessment of these parameters concurrently, thereby providing a broader and more comprehensive understanding of their impact on overall heat transfer effectiveness. The analysis covers a wide range of Reynolds numbers (1000, 2000, 3000, and 4000), hot fluid inlet temperatures (25°C, 30°C, 35°C, and 40°C), porous layer thicknesses (5/80, 10/80, 15/80, and 20/80), and porosity ratios (0.5, 0.6, 0.8, and 0.9). The results are compared with those obtained from non-porous tubes to comprehensively assess the influence of the porous structure on the thermal performance of the shell-and-tube heat exchanger.

2 Materials and Methods

2.1 Experimental Setup

The shell-and-tube heat exchanger employed in this research, as illustrated in Figure 1, features a circular tube arrangement consisting of six tube passes and a single shell pass. The exchanger incorporates four baffles placed along the shell to regulate the fluid flow and enhance heat transfer. Each tube within the shell has an inner diameter of 7 mm, an outer diameter of 8 mm, and a total length of 350 mm. Both the tubes and baffles were fabricated from 304 stainless steel to ensure durability and corrosion resistance, whereas the shell was constructed from transparent polycarbonate material to allow visual inspection during operation. The shell itself has an inner diameter of 70 mm and an outer diameter of 80 mm, while the distance between consecutive baffles is 70 mm. The baffles possess a geometric shape ratio of 20%, designed to promote efficient fluid redirection and improved mixing within the shell side.

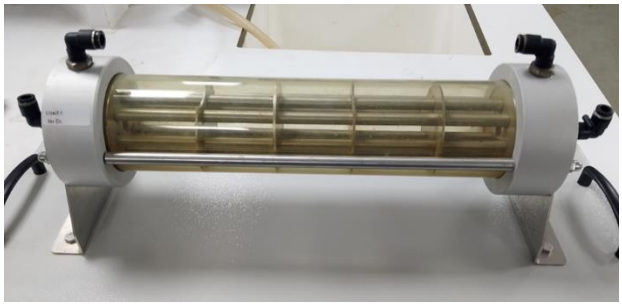

Figure 1. Shell and tube heat exchanger [22].

Within the experimental setup, the working fluid configuration consists of hot water flowing inside the tubes and cold water circulating around them on the shell side in a counterflow pattern to enhance thermal exchange efficiency. The hot-side flow operates under laminar conditions, with Reynolds numbers ranging between 1000 and 4000. During operation, the inlet temperature of the hot stream is fixed at 40°C, while the cold stream entering the shell side is maintained at 20°C. To establish a uniform thermal boundary condition, the heat required for the process is provided by electrically powered resistance elements connected to a controlled power unit that ensures a steady heat flux across the system, as shown in Figure 2.

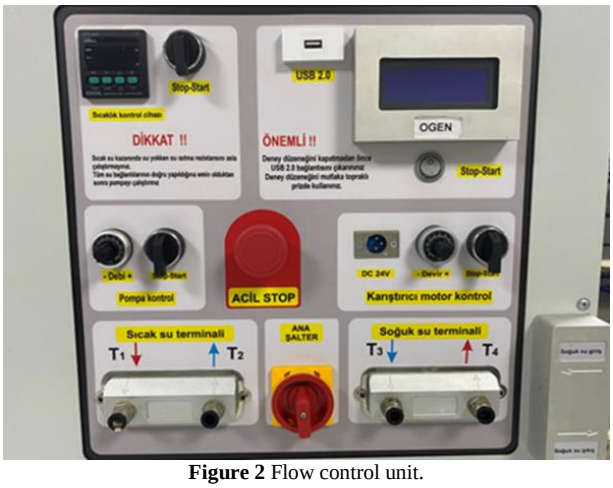

Figure 2 Flow control unit.

The thermal–hydraulic control unit used in the experimental setup enables precise adjustment of the hot fluid temperature and flow rate within a wide operating range. The system can regulate the fluid temperature between 15°C and 60°C, while the volumetric flow rate can be adjusted from 0.1 L/min up to 20 L/min. The internal thermostat ensures that the selected temperature remains constant during operation, preventing undesirable fluctuations. Additionally, real-time temperature measurements are obtained through integrated Type-K thermocouples (Nickel-Chromium / Nickel-Aluminum), which provide reliable sensing performance within the range of –200°C to +1260°C. This control system allows stable experimental conditions and accurate monitoring of thermal parameters throughout the measurements.

During the experiments, the flow rates of hot and cold fluids, as well as the inlet and outlet temperatures, were recorded using a data logging computer (Figure 3).

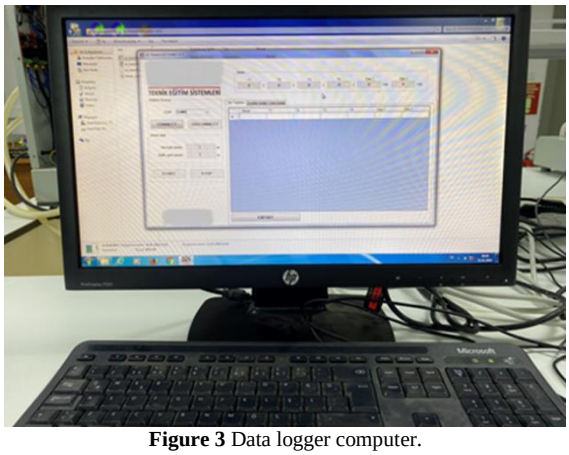

Figure 3 Data logger computer.

The experimental data acquisition and logging were performed using an HP Compaq Elite 8300 SFF workstation (Hewlett-Packard Company) equipped with an Intel Core i5-3470 CPU operating at 3.20 GHz and 4.0 GB of RAM under a 64-bit operating system. This computer served as the data logger for collecting temperature, flow rate, and system parameters throughout the experiment, and all measurements were recorded at a frequency of one sample per second to ensure high-resolution temporal tracking of system behavior, guaranteeing stable recording performance and uninterrupted data storage during all test procedures.

2.2 Numerical Model

A numerical analysis was carried out to complement the experimental study and to provide a clearer understanding of the heat exchanger's thermal and flow behavior. Using ANSYS Fluent, a three-dimensional model was developed to simulate heat transfer and fluid motion under the same operating conditions as the experiments. The computational domain was carefully constructed to capture the complex interactions between the shell-side and tube-side fluids, ensuring accurate representation of convective heat transfer. Boundary conditions such as inlet velocity, temperature, and wall heat flux were defined based on experimental data to maintain consistency between both approaches. This

numerical framework made it possible to evaluate velocity distributions, temperature gradients, and pressure variations throughout the exchanger, providing valuable insight into the effects of flow structure on thermal performance.

The mesh convergence analysis presented in Table 1 confirms that the numerical solution is not sensitive to further refinement beyond Model 6. As the element number increases from approximately 3.0×10^5 to 1.4×10^6, the average orthogonal quality improves from 0.740 to 0.880, while the average skewness decreases from 0.240 to 0.135. Notably, after Model 6, variations in both metrics become minimal, indicating diminishing returns from additional mesh refinement.

Table 1. The parameters for numerical analysis.

Model No	Element Number	Avg. Ort. Quality	Avg. Skewness
1	305916	0,740	0,240
2	424621	0,780	0,205
3	619793	0,810	0,182
4	633803	0,830	0,167
5	741030	0,845	0,158
6	891281	0,855	0,150
7	1026722	0,863	0,145
8	1102365	0,870	0,141
9	1236887	0,875	0,138
10	1400255	0,880	0,135

Therefore, Model 6 was selected for all subsequent numerical simulations, balancing computational efficiency and solution accuracy. This verification demonstrates that the computational model is mesh-independent and that the resulting fluid flow and heat transfer predictions are numerically robust. The mesh independence study was conducted by analyzing the variation of the hot fluid outlet temperature with respect to the total element number, as shown in Figure 4.

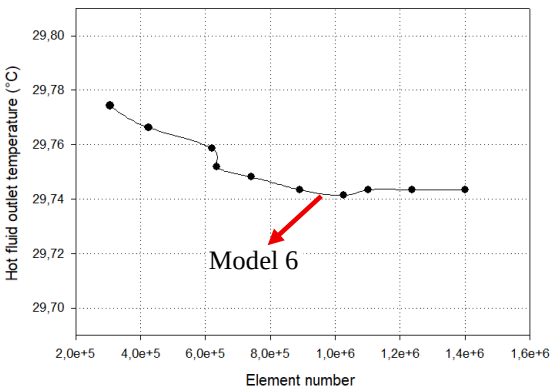

Figure 4 Element number against outlet temperature.

The results demonstrate that after Model 6 (approximately 1.0×10^6 elements), further refinement in mesh resolution produces negligible changes in the outlet temperature, confirming that the numerical results are mesh-independent. Therefore, Model 6 was selected for all subsequent simulations in the present study. This verification confirms that the numerical model is not sensitive to the mesh size, ensuring the reliability and stability of the computed results.

The governing equations used to describe the fluid flow and heat transfer processes are presented in Equations (1–5). The continuity equation, representing the conservation of mass, ensures that the net mass flux into and out of a control volume is balanced by the rate of mass accumulation or depletion occurring within that volume. Since the analyses in this study were performed under steady-state conditions, the temporal variation of density is assumed to be zero. Therefore, the mass inflow and outflow remain balanced throughout the domain, and the continuity equation can be expressed as follows:

$$\frac{\partial u}{\partial x}+\frac{\partial v}{\partial y}+\frac{\partial w}{\partial z}=0 \tag{1}$$

The momentum equation, derived from the conservation of momentum principle, defines the relationship between the acting forces and the resulting fluid motion. It incorporates the contributions of pressure gradients, viscous stresses, and body forces that influence the velocity distribution within the flow field. In the present study, steady-state flow conditions were assumed; hence, the transient term representing the temporal acceleration of the fluid was neglected. The resulting form of the momentum equation in the x, y and z-direction describes the balance between pressure forces, viscous effects, and inertial terms, and is expressed as follows:

$$u\frac{\partial u}{\partial x}+v\frac{\partial u}{\partial y}+w\frac{\partial u}{\partial z}=-\frac{1}{\rho}\frac{\partial p}{\partial x}+v\left[\frac{\partial^2 u}{\partial x^2}+\frac{\partial^2 u}{\partial y^2}+\frac{\partial^2 u}{\partial z^2}\right] \tag{2}$$

$$u\frac{\partial v}{\partial x}+v\frac{\partial v}{\partial y}+w\frac{\partial v}{\partial z}=-\frac{1}{\rho}\frac{\partial p}{\partial y}+v\left[\frac{\partial^2 v}{\partial x^2}+\frac{\partial^2 v}{\partial y^2}+\frac{\partial^2 v}{\partial z^2}\right] \tag{3}$$

$$u\frac{\partial w}{\partial x}+v\frac{\partial w}{\partial y}+w\frac{\partial w}{\partial z}=-\frac{1}{\rho}\frac{\partial p}{\partial z}+v\left[\frac{\partial^2 w}{\partial x^2}+\frac{\partial^2 w}{\partial y^2}+\frac{\partial^2 w}{\partial z^2}\right] \tag{4}$$

The energy equation represents the thermal behavior of the flow by quantifying the transfer and transformation of energy within the domain. It defines how the internal energy of the fluid changes as a result of heat conduction, convection, and viscous dissipation. Under steady-state conditions, the time-dependent variation of energy is neglected, and the equation simplifies to a balance between the net heat flux and the mechanical work acting on the fluid. The general form of the energy equation is expressed as follows:

$$u\frac{\partial T}{\partial x}+v\frac{\partial T}{\partial y}+w\frac{\partial T}{\partial z}=\alpha\left[\frac{\partial^2 T}{\partial x^2}+\frac{\partial^2 T}{\partial y^2}+\frac{\partial^2 T}{\partial z^2}\right] \tag{5}$$

The dimensionless number for Re (Reynolds) are described by the following general equation:

$$Re=\frac{\rho V D}{\mu} \tag{6}$$

In evaluating the thermal behavior of heat exchangers, the logarithmic mean temperature difference (LMTD) technique is one of the most established analytical tools used to determine the overall heat transfer performance. Rather than relying on a single temperature difference, this method incorporates the varying

temperature gradients between the two working fluids along the exchanger's length. By combining the inlet and outlet temperature differences in a logarithmic form, it provides a representative temperature potential that accurately characterizes the driving force for heat exchange. The calculated LMTD value, together with the overall heat transfer coefficient and the effective surface area, allows for a precise estimation of the total rate of heat transfer between the hot and cold fluids.

$$\Delta T_1 = T_{h,in} - T_{c,out} \tag{7}$$

$$\Delta T_2 = T_{h,out} - T_{c,in} \tag{8}$$

$$\Delta T_{lm} = \frac{\Delta T_1 - \Delta T_2}{\ln(\Delta T_1 / \Delta T_2)} \tag{9}$$

The specific heat capacity of a material represents its ability to store thermal energy, describing how much heat must be supplied to raise the temperature of a unit mass by one degree. This thermophysical property has a direct impact on how efficiently a substance can absorb or release heat, making it a fundamental factor in assessing the overall heat transfer characteristics and energy response of thermal systems [23]. Accurate determination of this parameter is essential for assessing the energy storage and transport characteristics of the working fluid.

$$C_c = \dot{m}_c c_{pc} \tag{10}$$

$$C_h = \dot{m}_h c_{ph} \tag{11}$$

The peak temperature of the system can be formulated mathematically to illustrate its dependence on thermal input, material characteristics, and boundary conditions.

$$\Delta T_{max} = T_{h,in} - T_{c,in} \tag{12}$$

$$\dot{Q}_{max} = C_{min} \Delta T_{max} \tag{13}$$

The heat transfer effectiveness can be mathematically formulated to relate the actual heat transfer rate to the maximum possible heat transfer achievable between the two working fluids.

$$\varepsilon = \frac{\dot{Q}_{act}}{\dot{Q}_{max}} = \frac{Actual\ heat\ transfer\ amount}{Maximum\ heat\ transfer\ amount} \tag{14}$$

The model geometry which has 350 mm length of shell and tubes, with the tubes arranged in a circular pattern, 80 mm outer diameter of the shell, 70 mm inner diameter of the shell, 7 mm inner diameter of tubes, 8 mm outer diameter of tubes is presented in Figure 5.

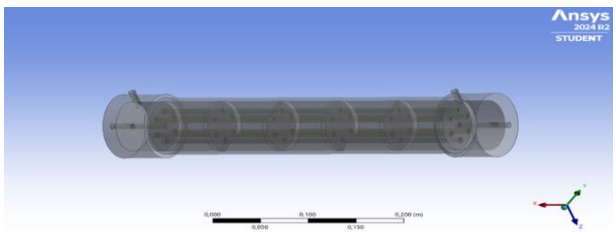

Figure 5 Geometry of the numerical model.

The model cross-section view of the shell and tube heat exchanger is presented to show internal components of shell and tube heat exchanger. The model cross-section view is presented in Figure 6.

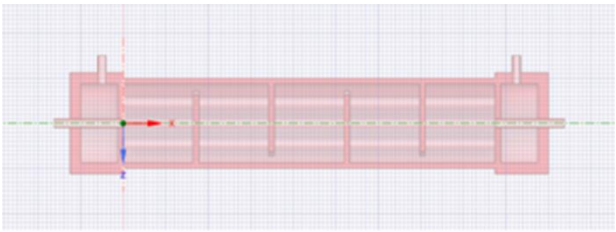

Figure 6 Cross section view in xz – direction.

As seen in Figure 7, three boundary layers are defined in the computational domain. The mesh elements are primarily concentrated near the solid–liquid interfaces, where boundary layer effects are more pronounced. Therefore, a higher mesh density is applied in these regions to ensure accurate resolution of the temperature and velocity gradients.

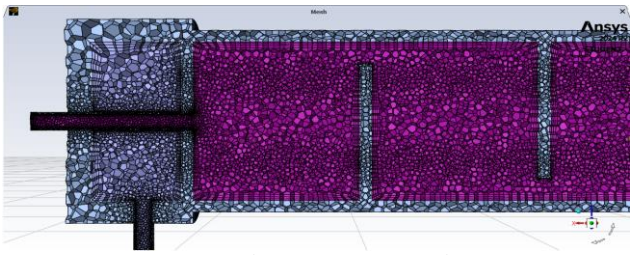

Figure 7 Mesh structure of the numerical model from cross section view.

Table 2. The parameters for numerical analysis.

Parameters	Constant variables	Definition
Re_{hot}=1000 =2000 =3000 =4000	$T_{h,in}$=45°C $T_{c,in}$=20°C Re_{cold}=2000	Reynolds number is increased from 1000 to 4000 in increments of 1000.
$T_{h,in}$=25°C =30°C =35°C =40°C	$T_{c,in}$=20°C Re_{hot}=4000 Re_{cold}=2000	Hot inlet temperature is increased from 25 to 40.
L/D =5/80 =10/80 =15/80 =20/80	$T_{h,in}$=40°C $T_{c,in}$=20°C Re_{hot}=1000 Re_{cold}=2000	Porous thickness is increased from 5/80 to 20/80 in increments.
Φ = 0.5 = 0.6 = 0.8 = 0.9	$T_{h,in}$= 40°C $T_{c,in}$= 20°C Re_{hot}= 1000 Re_{cold}= 2000	Porosity ratio is increased from 0.5 to 0.9.

Table 2 presents the parameters analyzed in the numerical study along with the corresponding constant variables. In each case, a single parameter was varied while the others were kept constant to isolate its effect on heat transfer effectiveness. The parameters investigated include Reynolds number, hot fluid inlet temperature, porous layer thickness, and porosity ratio.

3 Results and Discussions

This study investigates the heat transfer rate of water flowing through tubes containing porous media under laminar flow conditions. The effects of different Reynolds numbers (1000, 2000, 3000, and 4000), hot fluid inlet temperatures (25°C, 30°C, 35°C, and 40°C), porous layer thicknesses (5/80, 10/80, 15/80, and 20/80), and porosity ratios (0.5, 0.6, 0.8, and 0.9) were examined. Throughout the experiments, the inlet temperature of the cold fluid was kept constant at 20°C, and the Reynolds number on the cold side was maintained at 2000. The influence of these parameters on the heat transfer rate was investigated experimentally, while ANSYS was employed to numerically model the same conditions. The experimental results were used to validate the numerical findings.

3.1 Effect of Reynold Number on Heat Transfer Effectiveness

In the experimental setup, the heat transfer effectiveness of the hot fluid at an inlet temperature of 40°C was examined for different Reynolds numbers (1000, 2000, 3000, and 4000). When the Reynolds number increased from 1000 to 2000, the heat transfer effectiveness improved by 9.7%. A further increase from 2000 to 3000 resulted in an additional enhancement of 3.1%, while no significant change was observed between 3000 and 4000. Overall, a total increase of 12.8% in heat transfer effectiveness was recorded as the Reynolds number rose from 1000 to 4000.

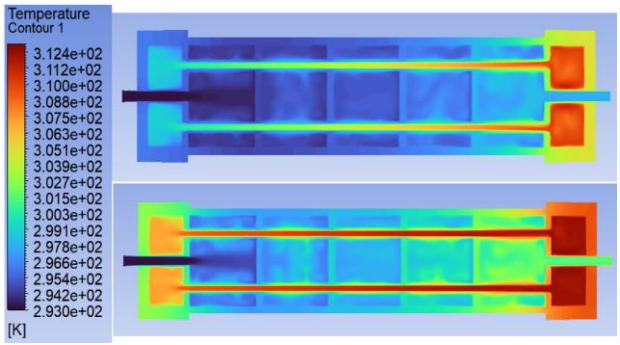

Figure 8 Temperature contours for Re= 1000 (upper) and Re= 4000.

Similarly, in the numerical analysis, the heat transfer effectiveness of the hot fluid at 40°C was evaluated for the same range of Reynolds numbers. An increase in the Reynolds number from 1000 to 2000 enhanced the effectiveness by 16.8%, followed by increases of 8.1% and 5.5% for the transitions from 2000 to 3000 and from 3000 to 4000, respectively. Overall, a total enhancement of 30.4% in heat transfer effectiveness was obtained in the numerical model. Figure 8 illustrates the temperature distribution for Re = 1000 and Re = 4000, whereas Figure 10 depicts the variation of heat transfer effectiveness with respect to the Reynolds number. The comparison between experimental and numerical findings demonstrated strong consistency, verifying the reliability and accuracy of the developed numerical model.

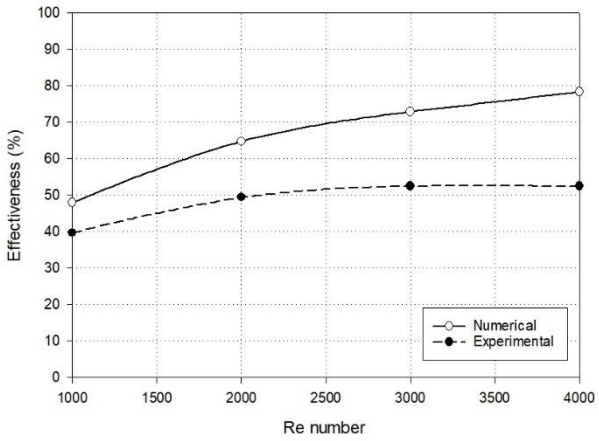

Figure 9 Effect of Reynolds number on heat transfer effectiveness.

Both experimental and numerical results (Figure 9) indicate that the effectiveness increases with increasing Reynolds number due to improved convective heat transfer at higher flow velocities. However, the numerical results exhibit higher effectiveness values compared to the experimental data, which can be attributed to idealized boundary conditions and the absence of certain heat losses in the numerical model.

3.2 Effect of Hot Inlet Temperature on Heat Transfer Effectiveness

In the experimental setup, the heat transfer effectiveness of the hot fluid at Re = 4000 was examined for different inlet temperatures (25°C, 30°C, 35°C, and 40°C). As the hot fluid inlet temperature increased from 25°C to 30°C, the heat transfer effectiveness improved by 0.5%. A further increase from 30°C to 35°C resulted in a 0.6% enhancement, while an additional rise from 35°C to 40°C increased the effectiveness by 0.3%. Overall, a total improvement of 1.4% in heat transfer effectiveness was observed as the inlet temperature increased from 25°C to 40°C.

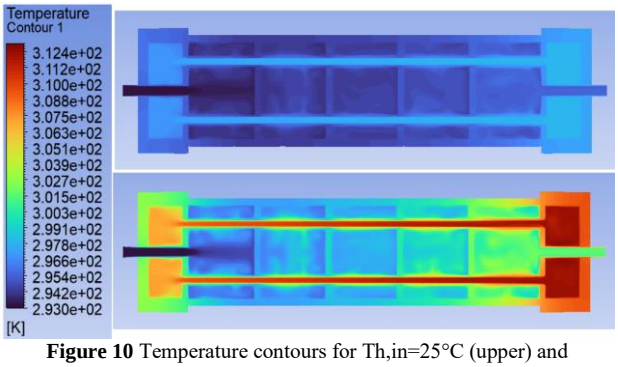

Figure 10 Temperature contours for Th,in=25°C (upper) and Th,in=40°C.

Similarly, in the numerical analysis, the heat transfer effectiveness of the hot fluid at Re = 4000 was evaluated for the same range of inlet temperatures. An increase from 25°C to 30°C enhanced the effectiveness by 0.5%, followed by increases of 0.7% and 0.7% for the ranges of 30°C–35°C and 35°C–40°C, respectively. In total, a 1.9% increase in heat transfer effectiveness was obtained numerically. The temperature contours for Th,in = 25°C and Th,in = 40°C are presented in Figure 10, while the variation of heat transfer effectiveness with different inlet

temperatures is shown in Figure 11. The numerical results exhibited good agreement with the experimental data, confirming the reliability of the numerical model.

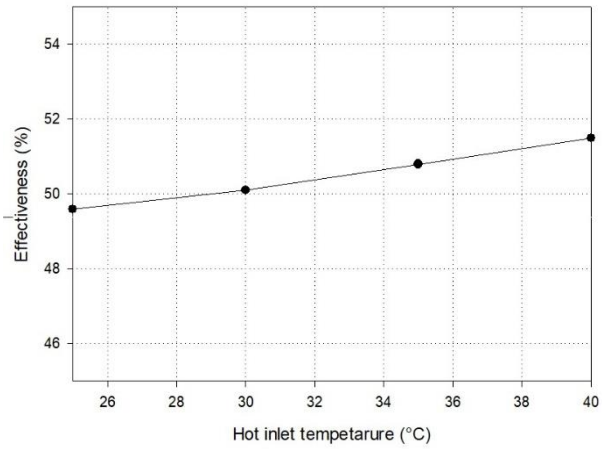

Figure 11 Effect of hot inlet temperature on heat transfer effectiveness.

This behavior can be attributed to the higher temperature difference between the hot and cold fluids, which enhances the driving potential for heat transfer. However, the increase is relatively small, indicating that within the tested temperature range, the dominant factor affecting heat transfer remains the flow characteristics rather than temperature variation alone.

3.3 Effect of Porosity Ratio on Heat Transfer Effectiveness

The heat transfer effectiveness of the hot fluid at 40°C and Re = 1000 was examined for different porosity ratios (0.5, 0.6, 0.8, and 0.9). Increasing the porosity ratio from 0.5 to 0.6 resulted in a 0.7% improvement in heat transfer effectiveness, while further increases from 0.6 to 0.8 and from 0.8 to 0.9 enhanced the effectiveness by 0.4% and 0.2%, respectively. In general, the heat transfer effectiveness exhibited a steady improvement as the porosity ratio increased from 0.5 to 0.9. Figure 12 presents the temperature contours corresponding to Φ = 0.5 and Φ = 0.9, while Figure 13 illustrates how heat transfer effectiveness varies with different porosity ratios.

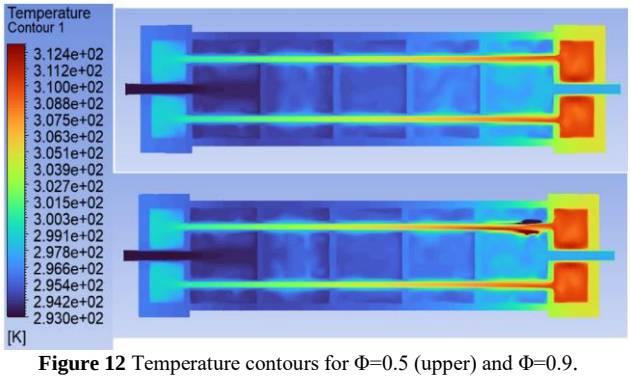

Figure 12 Temperature contours for Φ=0.5 (upper) and Φ=0.9.

As the porosity increases, the temperature distribution becomes more uniform due to improved fluid permeability and enhanced mixing within the porous medium. At lower porosity, flow resistance is higher, leading to localized hot regions near the tube wall and a less homogeneous temperature field. In contrast, at higher porosity, the fluid moves more freely through the porous region, resulting in a smoother thermal gradient and more effective heat transfer between the solid and fluid phases. This improvement in flow uniformity and heat exchange contributes to the observed increase in overall heat transfer effectiveness.

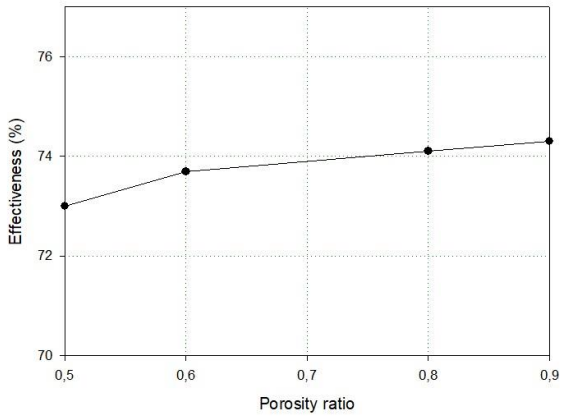

Figure 13 Effect of porosity ratio on heat transfer effectiveness.

Higher porosity enhances fluid permeability and promotes better flow distribution, resulting in improved convective heat transfer between the solid and fluid regions. However, the rate of increase becomes smaller at higher porosity values, indicating that beyond a certain point, the positive effect of increased permeability on heat transfer becomes limited.

3.4 Effect of Porous Thickness on Heat Transfer Effectiveness

The heat transfer effectiveness of the hot fluid at 40°C and Re = 1000 was examined for different porous thicknesses (5/80, 10/80, 15/80, and 20/80). Increasing the porous thickness from 5/80 to 10/80 improved the heat transfer effectiveness by 0.5%, while further increases from 10/80 to 15/80 and from 15/80 to 20/80 enhanced it by 0.4% and 1.3%, respectively. A total enhancement of 2.2% in heat transfer effectiveness was recorded as the porous thickness increased from 5/80 to 20/80. Figure 14 displays the temperature contours for L/D = 5/80 and L/D = 20/80, while Figure 15 illustrates the variation in heat transfer effectiveness corresponding to different porous thickness values.

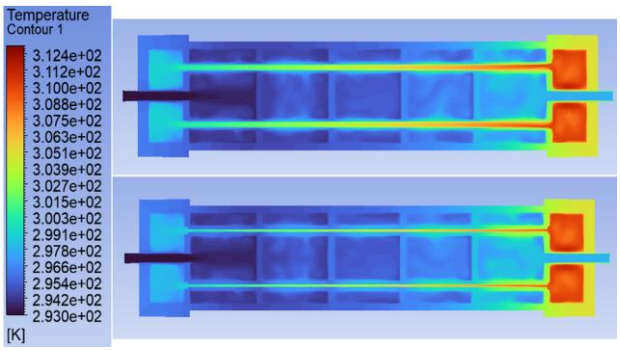

Figure 14 Temperature contours for L/D=5/80 (upper) and L/D=20/80.

This improvement in temperature uniformity reflects an increase in convective heat transfer and results in higher heat transfer effectiveness.

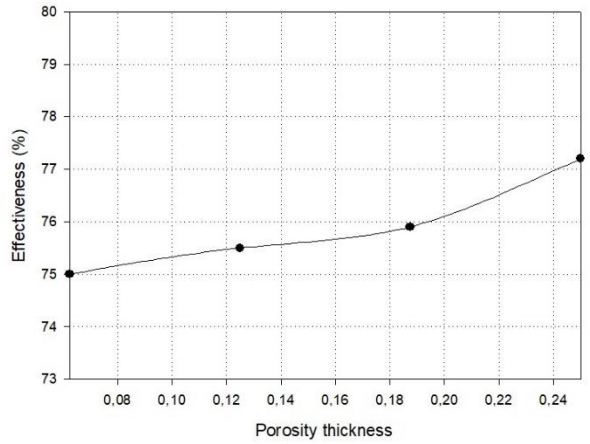

Figure 15 Effect of porosity thickness on heat transfer effectiveness.

This enhancement is attributed to the larger heat transfer surface area and improved interaction between the fluid and the porous medium, which promote greater energy exchange. The most significant improvement is observed at higher thickness values, where the extended contact surface allows more efficient heat conduction and convection, leading to higher overall thermal performance.

4 Conclusion

In this study, the effects of Reynolds number, hot fluid inlet temperature, porosity ratio, and porous thickness on the heat transfer performance of a shell-and-tube heat exchanger under laminar flow conditions were experimentally and numerically investigated. The numerical analysis conducted in ANSYS Fluent was validated by the experimental results, demonstrating a strong correlation between both approaches. The findings emphasize the impact of flow characteristics and porous structural parameters on heat transfer effectiveness and provide useful insights for the development of more efficient and compact heat exchanger designs.

1. It was determined that increasing the Reynolds number of the hot fluid stepwise from 1000 to 4000 at a hot inlet temperature of 40°C resulted in a 30.4% increase in overall heat transfer effectiveness.
2. At a Reynolds number of 4000, an increase in the hot fluid inlet temperature from 25°C to 40°C led to a noticeable improvement in overall heat transfer effectiveness, with an enhancement of approximately 1.9%. This increase is attributed to the greater temperature difference between the hot and cold fluids, which enhances the driving potential for heat transfer. The higher inlet temperature also promotes improved thermal conductivity and convective interaction between the fluid and the porous medium, resulting in more efficient heat exchange.
3. At a Reynolds number of 1000, with the hot fluid temperature kept constant at 40°C and a porous thickness ratio of 5/80, it was observed that decreasing the porosity ratio from 0.9 to 0.5 reduced the heat transfer effectiveness. It was determined that this reduction in porosity ratio resulted in an overall decrease of 1.3% in heat transfer effectiveness.
4. At a Reynolds number of 1000, with the hot fluid temperature kept constant at 40°C and a porosity ratio of 0.5, it was determined that increasing the porous thickness from 5/80 to 20/80 increased the overall heat transfer effectiveness by 2.2%.

Abbreviations

CH-STHE	Continuous helical shell and tube heat exchanger
CR	Circular ring
CRH	Circular ring with holes
CSS	Conventional single segmental
DSG-STHE	Double segmental shell and tube heat exchanger
DTP-STHE	Double-tube-pass shell and tube heat exchanger
HS	Hybrid segmental
LMTD	Logarithmic mean temperature difference
PB-STHE	Plate baffle shell and tube heat exchanger
RB-STHE	Rod baffle shell and tube heat exchanger
SG-STHE	Segmental shell and tube heat exchanger
STHE	Shell and tube heat exchanger
STP-STHE	Single-tube-pass shell and tube heat exchanger
ST-STHE	Staggered baffle shell and tube heat exchanger
TFB-STHE	Triple-layer flower baffle shell and tube heat exchanger
THB-STHE	Trefoil-hole baffle shell and tube heat exchanger

Declaration

Ethics committee approval is not required.

References

[1] Mohammadi, M. H., Abbasi, H. R., Yavarinasab, A., & Pourrahmani, H. (2020). Thermal optimization of shell and tube heat exchanger using porous baffles. *Applied Thermal Engineering*, 170, 115005.

[2] Rashidian, S., & Tavakoli, M. R. (2017). Using porous media to enhancement of heat transfer in heat exchangers. *International Journal of Advanced Engineering, Management and Science*, 3(11), 239937.

[3] Abbasi, H. R., Sedeh, E. S., Pourrahmani, H., & Mohammadi, M. H. (2020). Shape optimization of segmental porous baffles for enhanced thermo-hydraulic performance of shell-and-tube heat exchanger. *Applied Thermal Engineering*, 180, 115835.

[4] Tian, H., Zhao, T., Shi, L., Chen, T., Ma, X., Zhang, H., & Shu, G. (2020). Assessment and optimization of exhaust gas heat exchanger with porous baffles and porous fins. *Applied Thermal Engineering*, 178, 115446.

[5] Wang, X., Zheng, N., Liu, Z., & Liu, W. (2018). Numerical analysis and optimization study on shell-side performances of a shell and tube heat exchanger with staggered baffles. *International Journal of Heat and Mass Transfer*, 124, 247-259.

[6] Rad, S. E., Afshin, H., & Farhanieh, B. (2015). Heat transfer enhancement in shell-and-tube heat exchangers using porous media. *Heat Transfer Engineering*, 36(3), 262-277.

[7] Marzouk, S. A., Abou Al-Sood, M. M., El-Said, E. M., Younes, M. M., & El-Fakharany, M. K. (2023). A comprehensive review of methods of heat transfer enhancement in shell and tube heat exchangers. Journal of Thermal Analysis and Calorimetry, 148(15), 7539-7578.

[8] You, Y., Fan, A., Lai, X., Huang, S., & Liu, W. (2013). Experimental and numerical investigations of shell-side thermo-hydraulic performances for shell-and-tube heat exchanger with trefoil-hole baffles. *Applied Thermal Engineering*, 50(1), 950-956.

[9] Bichkar, P., Dandgaval, O., Dalvi, P., Godase, R., & Dey, T. (2018). Study of shell and tube heat exchanger with the effect of types of baffles. *Procedia Manufacturing*, 20, 195-200.

[10] Wen, J., Yang, H., Wang, S., Xue, Y., & Tong, X. (2015). Experimental investigation on performance comparison for shell-and-tube heat exchangers with different baffles. *International Journal of Heat and Mass Transfer*, 84, 990-997.

[11] Wang, X., Zheng, N., Liu, Z., & Liu, W. (2018). Numerical analysis and optimization study on shell-side performances of a shell and tube heat exchanger with staggered baffles. *International Journal of Heat and Mass Transfer*, 124, 247-259.

[12] Chen, J., Zhao, P., Wang, Q., & Zeng, M. (2021). Experimental investigation of shell-side performance and optimal design of shell-and-tube heat exchanger with different flower baffles. *Heat Transfer Engineering*, 42(7), 613-626.

[13] Nie, C., Chen, Z., Liu, X., Li, H., Liu, J., & Rao, Z. (2024). Design of metal foam baffle to enhance the thermal-hydraulic performance of shell and tube heat exchanger. *International Communications in Heat and Mass Transfer*, 159, 108005.

[14] Cao, Y., Ke, H., Klemeš, J. J., Zeng, M., & Wang, Q. (2021). Comparison of aerodynamic noise and heat transfer for shell-and-tube heat exchangers with continuous helical and segmental baffles. *Applied Thermal Engineering*, 185, 116341.

[15] Yang, J., & Liu, W. (2015). Numerical investigation on a novel shell-and-tube heat exchanger with plate baffles and experimental validation. *Energy conversion and management*, 101, 689-696.

[16] He, L., & Li, P. (2018). Numerical investigation on double tube-pass shell-and-tube heat exchangers with different baffle configurations. *Applied Thermal Engineering*, 143, 561-569.

[17] He, S., Wang, M., Tian, W., Qiu, S., & Su, G. H. (2022). Development of an OpenFOAM solver for numerical simulations of shell-and-tube heat exchangers based on porous media model. *Applied Thermal Engineering*, 210, 118389.

[18] Riyadi, T. W., Herawan, S. G., Tirta, A., Ee, Y. J., Hananto, A. L., Paristiawan, P. A., ... & Veza, I. (2024). Nanofluid heat transfer and machine learning: Insightful review of machine learning for nanofluid heat transfer enhancement in porous media and heat exchangers as sustainable and renewable energy solutions. *Results in Engineering*, 24, 103002.

[19] Moraga, N. O., Rosas, C. E., Bubnovich, V. I., & Tobar, J. R. (2009). Unsteady fluid mechanics and heat transfer study in a double-tube air–combustor heat exchanger with porous medium. *International journal of heat and mass transfer*, 52(13-14), 3353-3363.

[20] Qader, F., Hussein, A. M., Danook, S. H., Mohamad, B., & Khaleel, O. S. (2023). Enhancement of double-pipe heat exchanger effectiveness by using porous media and TiO_2 water. *CFD Letters*, 15(4), 31-42.

[21] Juan, D., & Hai-Tao, Z. (2018). Numerical simulation of a plate-fin heat exchanger with offset fins using porous media approach. *Heat and Mass Transfer*, 54(3), 745-755.

[22] Kılıç, M., & Şahin, M. (2023). Nanoakışkan Hacimsel Oranının ve Parçacık Boyutunun Gövde Borulu Isı Değiştiricisindeki Isı Transferine Etkisinin Deneysel ve Sayısal İncelenmesi. *Çukurova Üniversitesi Mühendislik Fakültesi Dergisi,* 38(2), 531-543.

[23] Cengel, Y. A., & Ghajar, A. J. (2014). Heat and Mass Transfer (in SI Units). *Mcgraw-Hill Education-Europe, London*.